

Abstract

A “Ribbon” of enhanced energetic neutral atom (ENA) emissions was discovered by the Interstellar Boundary Explorer in 2009, redefining our understanding of the heliosphere boundaries and the physical processes occurring at the interstellar interface. The Ribbon signal is intertwined with that of a globally distributed flux (GDF) that spans the entire sky.

To a certain extent, Ribbon separation methods enabled examining its evolution independent of the underlying GDF. Observations over a full solar cycle revealed the Ribbon’s evolving nature, with intensity variations closely tracking those of the solar wind (SW) structure after a few years delay, accounting for the SW–ENA recycling process.

In this work, we examine the Ribbon structure, namely its ENA fluxes, angular extent, width, and circularity properties for two years, 2009 and 2019, representative of the declining phases of two adjacent solar cycles. We find that, (i) the Ribbon ENA fluxes have recovered in the nose direction and south of it down to $\sim 25^\circ$ (for energies below 1.7 keV) and not at mid and high ecliptic latitudes; (ii) the Ribbon width exhibits significant variability as a function of azimuthal angle; (iii) circularity analysis suggests that the 2019 Ribbon exhibits a statistically consistent radius with that in 2009. The Ribbon’s partial recovery is aligned with the consensus of a heliosphere with its closest point being southward of the nose region. The large variability of the Ribbon width as a function of azimuth in 2019 compared to 2009 is likely indicative of small-scale processes within the Ribbon.

Motivation

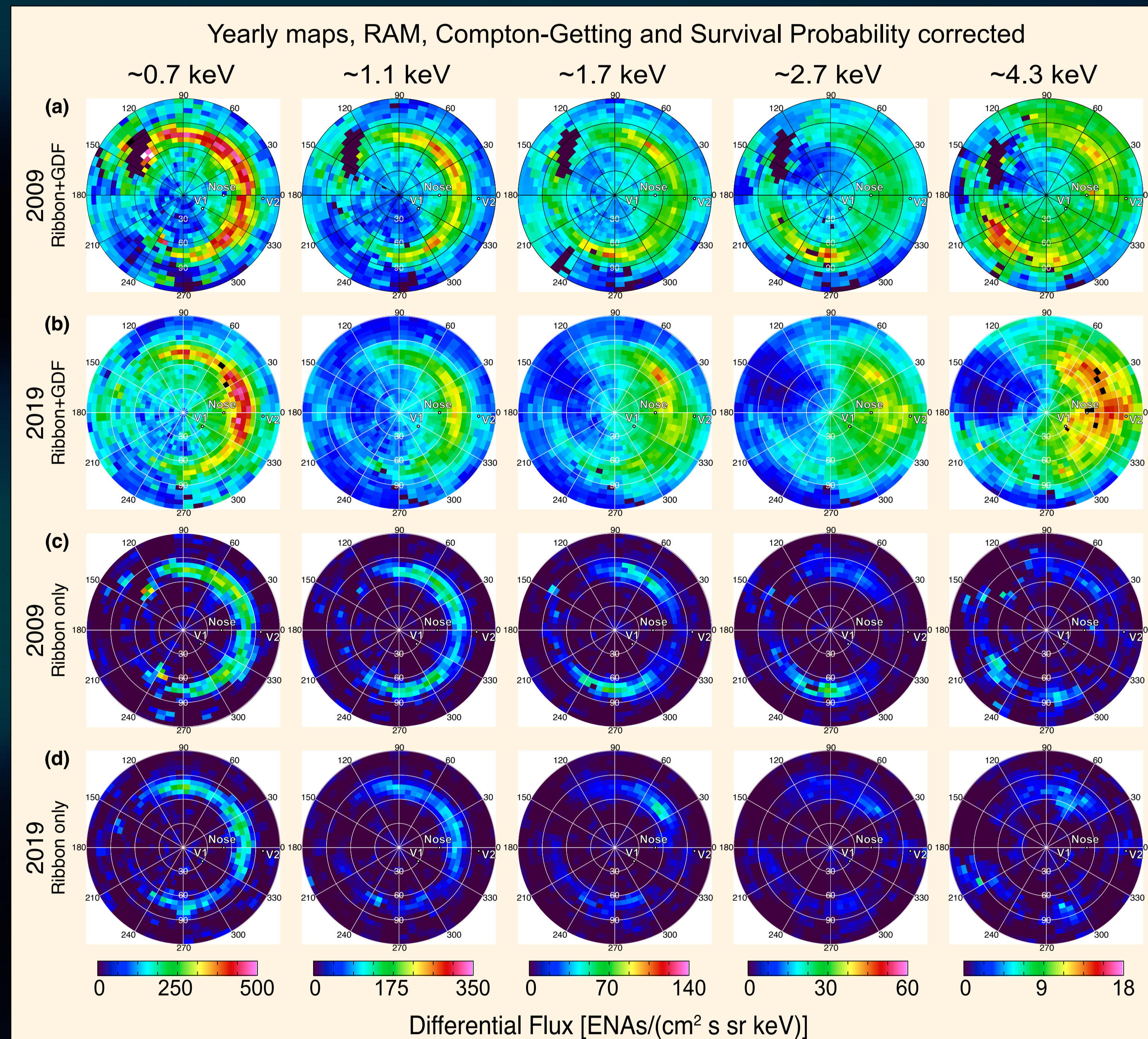


Figure 1. Ribbon-centered sky maps obtained by IBEX during 2009 and 2019, for five IBEX-Hi energy passbands (columns). Panels (a) and (b) show the full ENA signal of the Ribbon and the GDF. Panels (c) and (d) show the Ribbon-only signal obtained as a difference between the observations including both the GDF and Ribbon components and the GDF estimated as a linear combination of low-degree spherical harmonics Swaczyna et al. (2022). Consistent color-coding is shown for each energy passband for easy comparison. **The goal is to quantify Ribbon recovery over 11 years.**

Methodology

- Identify the Ribbon enhancement in the Ribbon maps between the polar angles of 45° and 110° .
- Determine boundaries by quantifying the signal above the statistical fluctuations, as:

$$J_{loc} + \frac{\sigma_{J_{loc}}}{2} \leq 0$$

where J_{loc} is the local flux of the Ribbon and $\sigma_{J_{loc}}$ is its uncertainty.

Also excluded are azimuths from the Ribbon-separated data that have originally missing pixels in the Ribbon region. All remaining Ribbon-only regions for all energies and azimuths are then used to assess the Ribbon structure recovery by deriving the three quantities defined below.

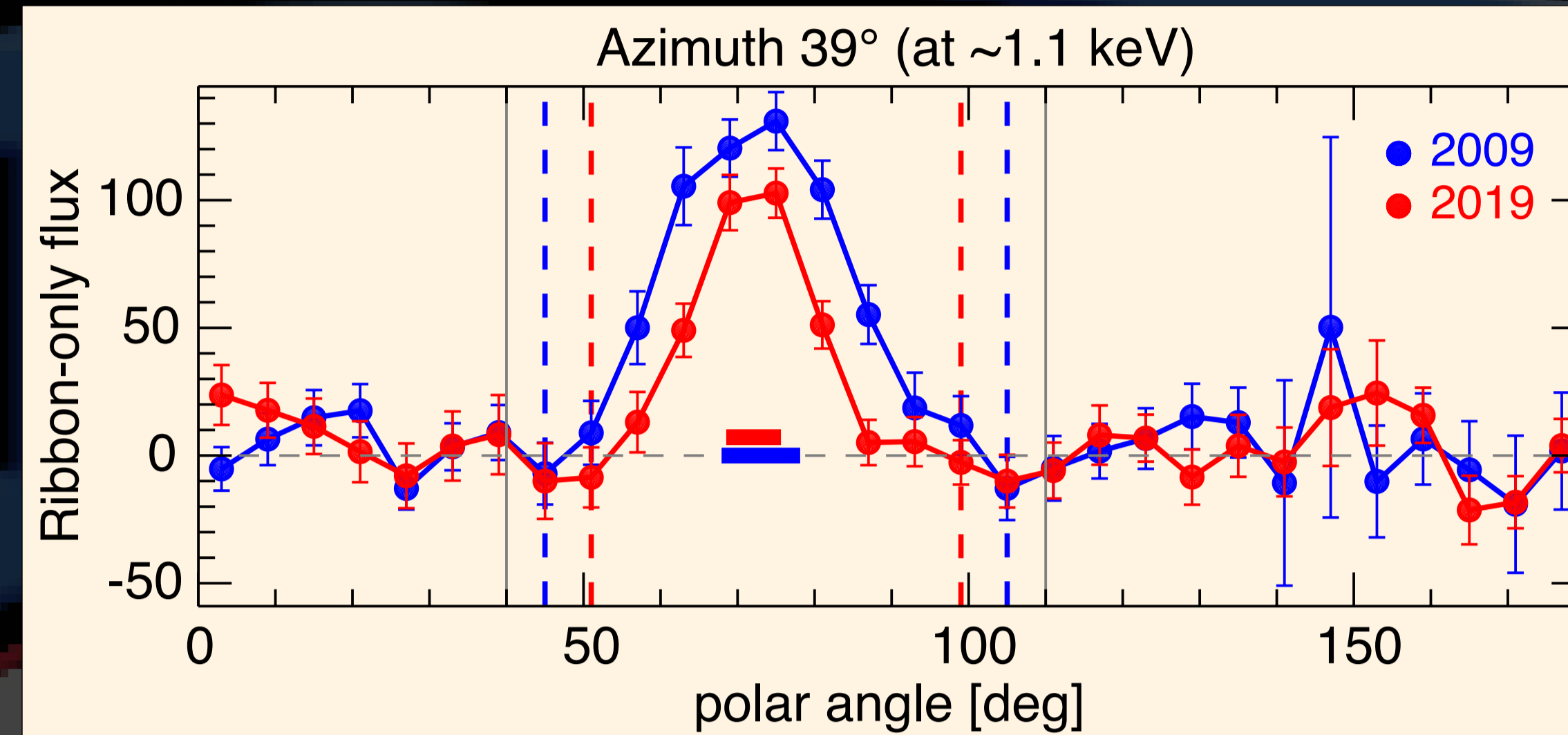


Figure 2. Illustration of Ribbon region determination used to assess its recovery.

- 1. Ribbon Integrated Flux:** This quantity measures the total flux under the Ribbon within the determined boundaries, as

$$J_R = \sum_i J_i$$

The integrated flux describes the changes of the total ENA intensity within the Ribbon.

- 2. Ribbon Angular Distance from the map center:** This indicates the Ribbon mean location away from the map center. It is defined as the first moment of the Ribbon profile weighted by the ENA fluxes within, given by

$$\varphi_R = \frac{\sum_i \theta_i J_i}{\sum_i J_i}$$

where j_i is the derived Ribbon flux at each polar angle θ_i .

- 3. Ribbon width, σ_R :** This quantity measures the 1σ width of the Ribbon, and is derived using the second central moment of the Ribbon distribution, and is given by,

$$\sigma_R = \sqrt{I_2 - \varphi_R^2}$$

where

$$I_2 = \frac{\sum_i \theta_i^2 J_i}{\sum_i J_i}$$

Results

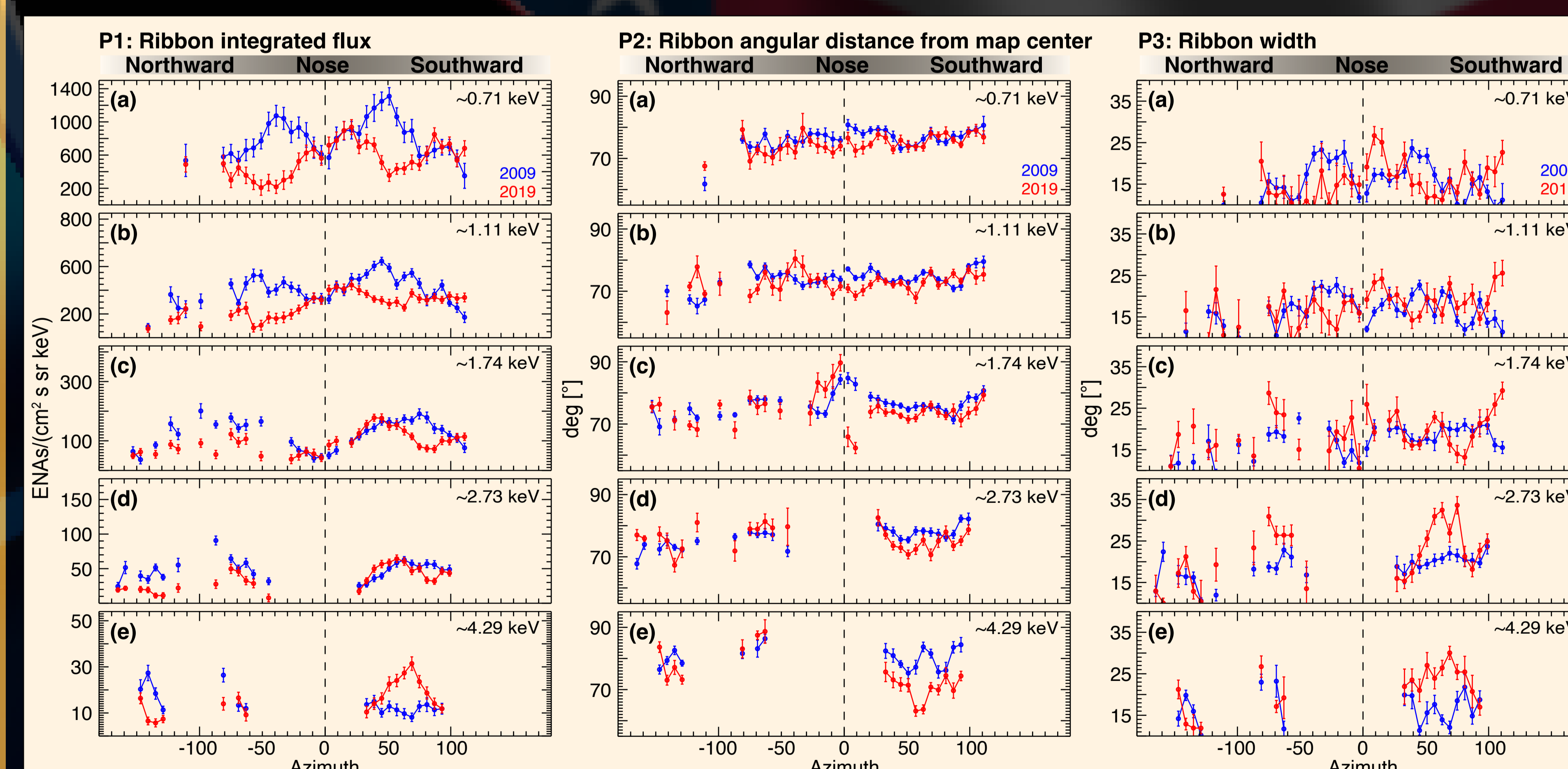


Figure 3. Derived properties of the Ribbon-only fluxes comparing 2009 and 2019. Trends show very interesting behavior of the Ribbon’s difference, most importantly that it varies at different rates away from the nose.

Results - Continued

Main findings:

1. Below ~ 1.7 keV, integrated Ribbon fluxes recover in the region from the nose to $\sim 25^\circ$ azimuth southward (Figure 3, P1(a)–(c)).

2. The Ribbon width exhibits significant variability as a function of azimuthal angle around the map center, with “out-of-phase” variability between 2009 and 2019. (P1(e), P2(e), P3(e)).

3. Circularity analysis shows that the 2019 Ribbon exhibits a statistically consistent radius with that in 2009 (Figure 5(b)).

Figure 4. Ribbon mean and width (i.e., “wedge”) locations plotted on a Ribbon-centered map for 2009 (left column), 2019 (middle column), and for both years (right column). Black dots and superimposed yellow error bars indicate the derived mean angular distances from the center and its uncertainty.

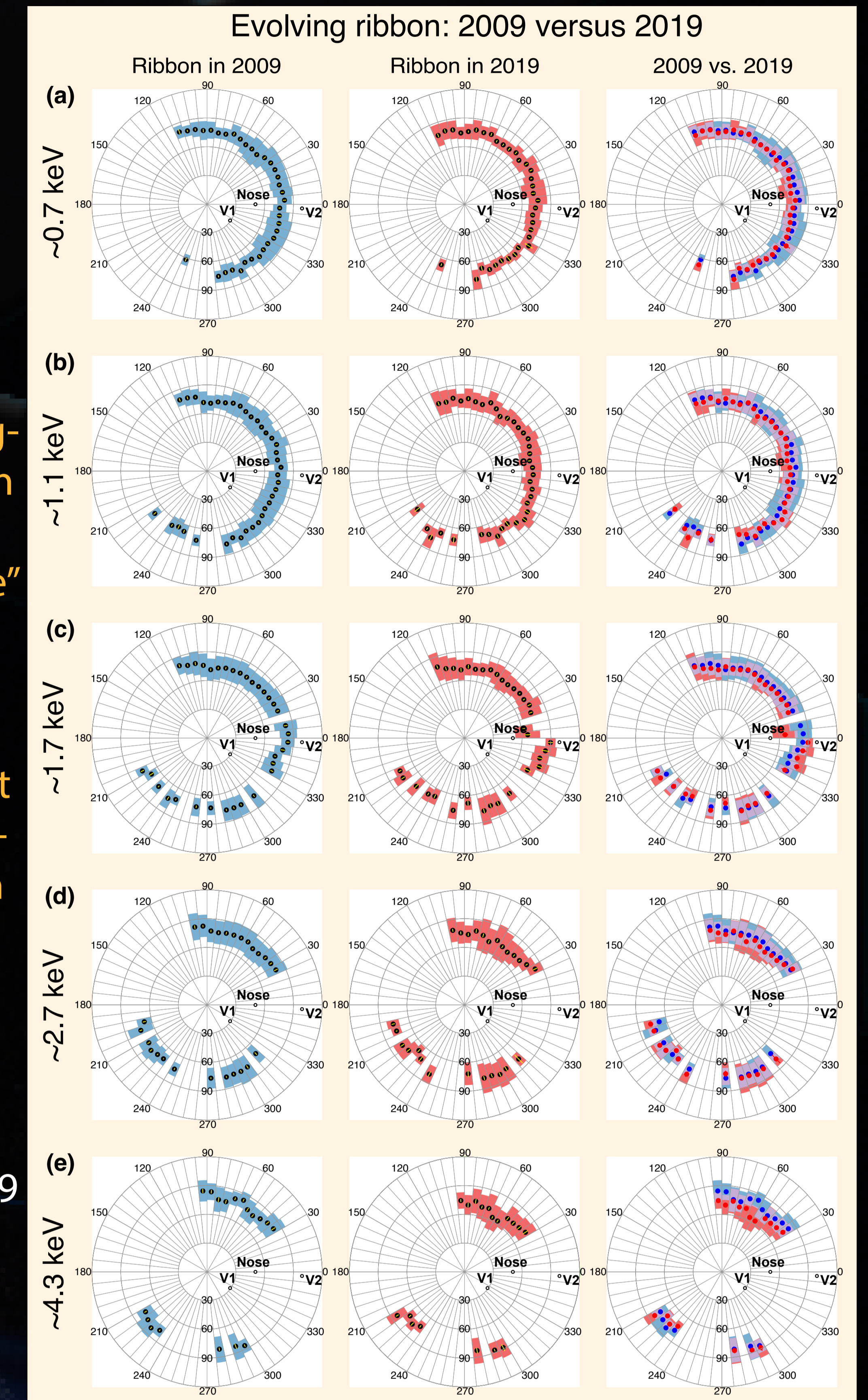
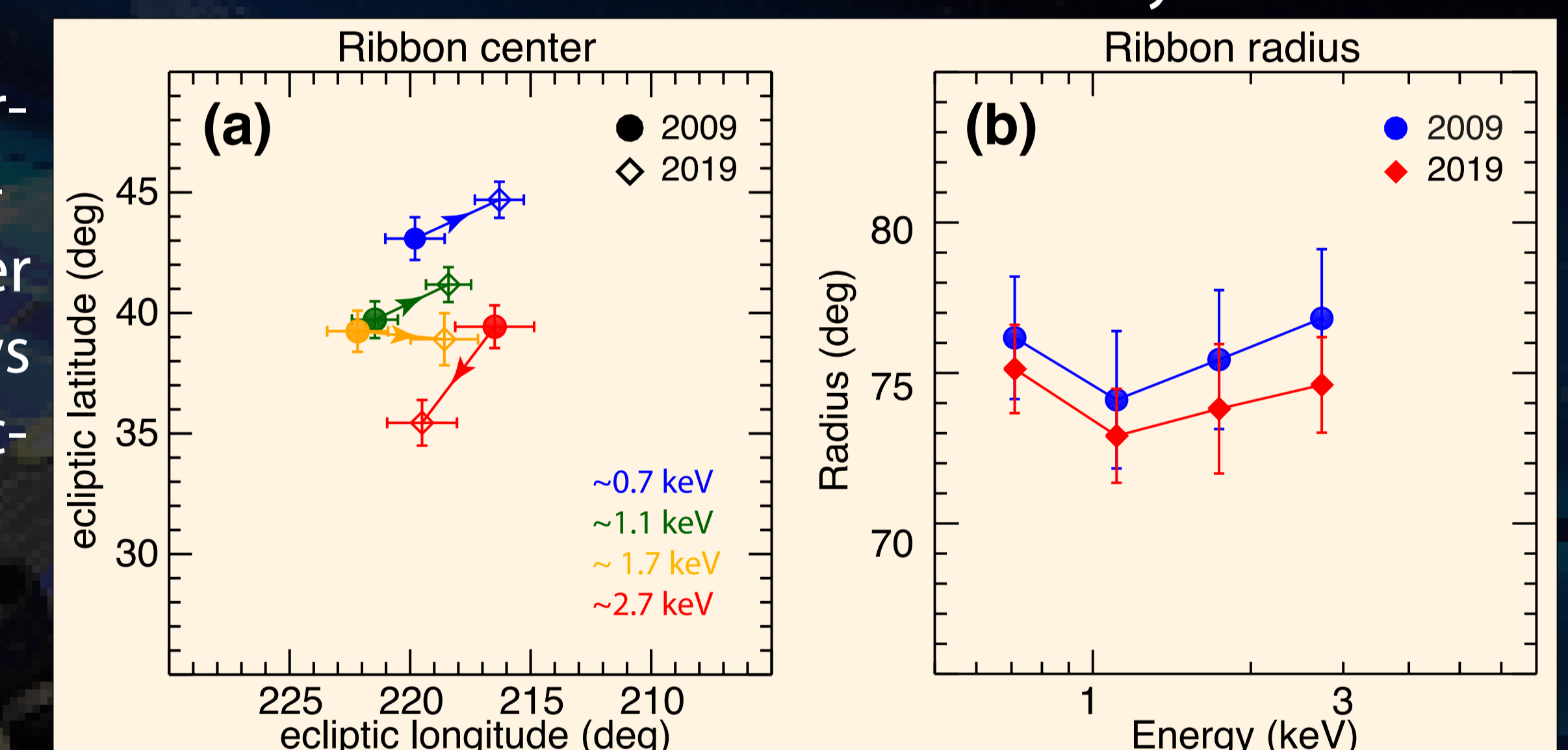


Figure 5. Results of the circularity analysis. (a) Variations of the derived center from 2009 to 2019. Arrows indicate the shifting direction. (b) Variations of the derived radius.



Circularity analysis was performed utilizing chi-square minimization to fit a circle to the Ribbon peak locations and their uncertainties, as described in Swaczyna et al. (2016), and Zirnstein et al. (2023). Results are shown in Figure 5 for four energy pass bands. The center of the Ribbon shifts to lower longitudes over time for the lowest three energy channels, but to a higher longitude for ~ 2.7 keV. Similarly for latitude, the center in 2019 is at a higher latitude (~ 0.7 and 1.1 keV) and at a lower latitude for ~ 2.7 keV, while the ~ 1.7 keV. Ribbon center latitude does not appear to change between 2009 and 2019. Ribbon radius in 2019 is systematically smaller than that of 2009, although they are still statistically consistent based on our uncertainty analysis.

Ribbon’s partial recovery is consistent with the consensus of a heliosphere with its closest point being southward of the nose region. The variability in the width as a function of azimuth is potentially indicative of small-scale variations within the Ribbon source region.

Article: Dayeh et al., ApJ, 952:19, 2023

Acknowledgements: NASA HGI-O grant 80NSSC21K0582. Also partial support through the IBEX mission under 80NSSC20K0719.